JOURNAL OF THE AMERICAN WATER RESOURCES ASSOCIATION

AMERICAN WATER RESOURCES ASSOCIATION

TWENTY-ONE-YEAR SIMULATION OF CHESAPEAKE BAY WATER QUALITY USING THE CE-QUAL-ICM EUTROPHICATION MODEL[1]

Carl F. Cerco and Mark R. Noel[2]

ABSTRACT: The CE-QUAL-ICM (Corps of Engineers Integrated Compartment Water Quality Model) eutrophication model was applied in a 21-year simulation of Chesapeake Bay water quality, 1985-2005. The eutrophication model is part of a larger model package and is forced, in part, by models of atmospheric deposition, watershed flows and loads, and hydrodynamics. Results from the model are compared with observations in multiple formats including time series plots, cumulative distribution plots, and statistical summaries. The model indicates only one long-term trend in computed water quality: light attenuation deteriorates circa 1993 through the end of the simulation. The most significant result is the influence of physical processes, notably stratification and associated effects (e.g., anoxic volume), on computed water quality. Within the application period, physical effects are more important determinants of year-to-year variability in computed water quality than external loads.

(KEY TERMS: transport and fate; eutrophication; simulation; Chesapeake Bay.)

Cerco, Carl F. and Mark R. Noel, 2013. Twenty-One-Year Simulation of Chesapeake Bay Water Quality Using the CE-QUAL-ICM Eutrophication Model. *Journal of the American Water Resources Association* (JAWRA) 1-15. DOI: 10.1111/jawr.12107

INTRODUCTION

Predictive models have been used to guide management of Chesapeake Bay almost since the inception of the Chesapeake Bay Program (CBP) in 1983. The initial multidimensional model of the bay (HydroQual Inc., 1987) revealed multiple deficiencies in contemporary modeling technology. These included lack of a predictive model of sediment diagenetic processes and inability to conduct continuous multiyear simulations. Initial nutrient reduction goals (40% reduction in nitrogen and phosphorus loads to the bay) (CBP, 1987) were formulated based on expert consensus and available models, but stakeholders recognized the need to reexamine the goals following the development of required technology. A basic model framework was established to meet the needs of the CBP and has been subject to continuous revision since then. Three major study phases preceded this one. The first phase (Cerco and Cole, 1993) provided modeling technology for the 1991 reevaluation of the 1987 nutrient reduction goals. The second phase (Cerco *et al.*, 2002) refined the computational grid to improve representation in the Virginia tidal tributaries and introduced living resources into the computational framework. This phase provided computational tools (Butt *et al.*, 2000) for the Tributary Strategy management effort. The third phase (Cerco and Noel, 2004) continued the grid refinements and extended the model into still smaller tributaries. This version of the model provided verification for a 2003 agreement

[1]Paper No. JAWRA-12-0063-P of the *Journal of the American Water Resources Association* (JAWRA). Received March 13, 2012; accepted August 31, 2012. **Discussions are open until six months from print publication**

[2]Research Hydrologist and Mathematician, US Army Engineer Research and Development Center, 3909 Halls Ferry Road, Vicksburg, Mississippi 39180 (E-Mail/Cerco: carl.f.cerco@usace.army.mil).

to cap annual average nitrogen and phosphorus loads to the bay. The present phase of the modeling effort commenced in 2004. The primary goal was to provide guidance for the development of Total Maximum Daily Loads (TMDLs) for the Chesapeake Bay and its watershed (USEPA, 2010). The TMDLs are intended to achieve water quality standards by removing impairments in three areas: dissolved oxygen (DO), water clarity, and chlorophyll (CHL) (USEPA, 2003).

CE-QUAL-ICM

The Corps of Engineers Integrated Compartment Water Quality Model (CE-QUAL-ICM or simply ICM) is part of a larger Chesapeake Bay Environmental Model Package which combines multiple interactive models. The Community Multiscale Air Quality Model (Dennis *et al.*, 2010) and a set of regression models (Grimm and Lynch, 2004) compute daily atmospheric nitrogen and phosphorus loads to the Chesapeake Bay watershed and to the water surface. The Watershed Model (WSM) (Shenk and Linker, this issue) provides daily computations of flow, solids loads, and nutrient loads at the heads of major tributaries and along the shoreline below the tributary inputs. Flows from the WSM are one set of inputs to the Computational Hydrodynamics in Three Dimensions (CH3D) hydrodynamic model (Kim, this issue). CH3D computes surface level, 3-D velocities, and vertical diffusion on a time scale measured in minutes. Loads from the WSM and transport processes from CH3D drive the CE-QUAL-ICM eutrophication model. ICM computes, in 3-D, physical properties, algal production, and elements of the aquatic carbon, nitrogen, phosphorus, silica, and oxygen cycles. These are computed on time scales of minutes although computations averaged up to longer time periods, hours to one day, are more representative of observations. ICM incorporates several submodels including sediment diagenesis (DiToro, 2001), submerged aquatic vegetation (SAV) (Cerco and Moore, 2001), and benthic invertebrates (Cerco and Meyers, 2000).

Several new capabilities were added to CE-QUAL-ICM to enhance management applicability during the TMDL development process. The previous computation of light attenuation via a partial attenuation model (Cerco *et al.*, 2004) was replaced by a model based on inherent optical properties including beam attenuation and scattering (Gallegos *et al.*, 2011). Parameters in the optical model were based on *in situ* measures, which related optical properties to environmental variables including color, CHL concentration, and suspended solids. The revised light attenuation model was intended to place the computation on a sound physical basis instead of relying on the empirical parameterization of the partial attenuation model.

Inorganic (fixed) solids for computation of light attenuation were provided by a fully predictive suspended solids module (Cerco *et al.*, 2010) which incorporated four classes of solids: fine clay, clay, silt, and sand. The module incorporated sediment resuspension based on shear stresses generated by tidal currents and wave action. Resuspension was included to avoid a perceived shortcoming with the previous model version (Cerco *et al.*, 2004) which relied on net settling to the sediments. In the previous version, a particle which settled to the bottom remained on the bottom. Although this approach provided good agreement between computed and observed solids, the potential existed for exaggeration of benefits from solids load reductions as the continuous source from resuspension was not considered.

The present CE-QUAL-ICM incorporates 36 state variables (Table 1) and operates on a computational grid of 50,000 cells (each 1,000 m $\times$ 1,000 m $\times$ 1.5 m) which extends from the mouth of the bay to the heads of tide of the bay and major tributaries (Cerco *et al.*, 2010). A Z-plane coordinate system is used in the vertical in which the number of layers varies from 1 to 19 according to local depth. Integration time step is five minutes although computations are typically averaged up to daily values before output from the model. Duration of the model simulations varied. Calibration was conducted in a continuous simulation of the years 1991-2000. Following calibration, the simulation was extended to 1985-2005 and results of that simulation are presented herein. We restrict attention to the main stem of the bay (Figure 1). System-wide model results are available in Cerco *et al.* (2010).

TABLE 1. CE-QUAL-ICM State Variables as Applied to Chesapeake Bay.

Salinity	Refractory particulate organic nitrogen
Temperature	Phosphate
Blue-green algae	Dissolved organic phosphorus
Spring diatoms	Labile particulate organic phosphorus
Green algae	Refractory particulate organic phosphorus
Microzooplankton	Particulate inorganic phosphorus
Mesozooplankton	Chemical oxygen demand
Dissolved organic carbon	Dissolved oxygen
Labile particulate organic carbon	Dissolved silica
Refractory particulate organic carbon	Particulate biogenic silica
Ammonium	Fine clay
Nitrate-nitrite	Clay
Dissolved organic nitrogen	Silt
Labile particulate organic nitrogen	Sand

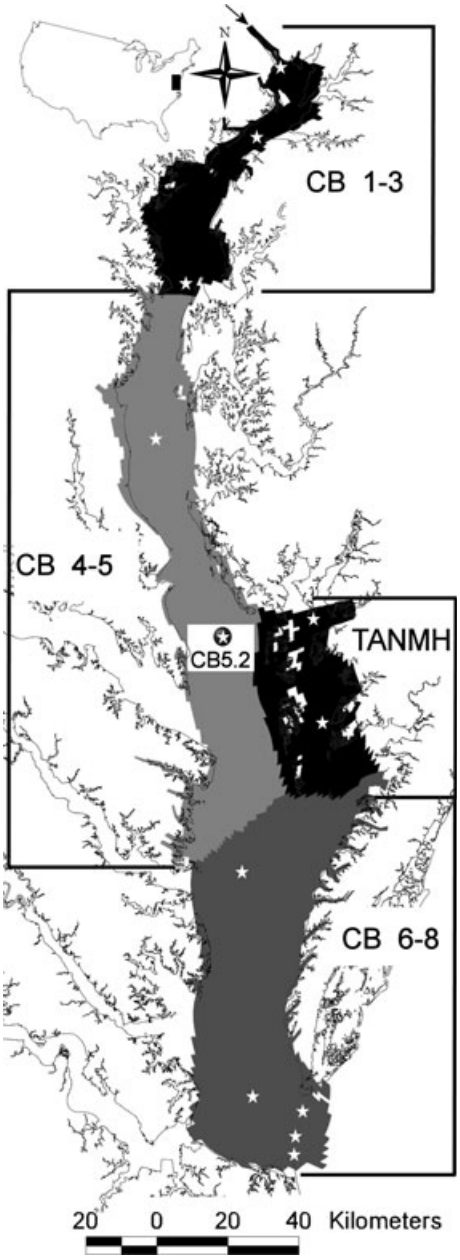

FIGURE 1. The Main Stem of Chesapeake Bay. This figure shows aggregation regions and sample stations considered in model-data comparisons (white stars). The entry point for Susquehanna River loads is indicated by the arrow at the top of the figure.

FORCING FUNCTIONS

Runoff

The Susquehanna drains a 70,000 km^2 watershed and empties into the bay at its northern extent (Figure 1). The river is by far the largest source of freshwater to the main stem bay and contributes 60% of the total freshwater flow to the bay and its tributaries (Chesapeake Bay River Input Monitoring Program. Accessed June 2012, http://va.water.usgs.gov/chesbay/RIMP/01578310.html). The preponderance of flow and associated loads occur during winter and spring although major flows can occur in late summer during tropical storm events. Winter/spring flows and loads are major influences on water quality during the SAV growing season and the period of summer hypoxia. The greatest winter/spring flows during the calibration period occur during the mid-1990s (Figure 2). The decade is unusual as it shows years of alternating extremes. The year 1995 has the least winter/spring runoff, whereas 1993 has the greatest. The period 1985-1992 is characterized by moderate flows and low variability. The 2000 decade commences with a drought in 2001 after which flows increase until the end of the simulation period.

Nutrient Loads

Nutrient loads (multiple forms of nitrogen and phosphorus) for this application are provided by Phase 5.3 of the Bay Program's WSM (Shenk and Linker, this issue). Loads from the watershed above the head of tide on major tributaries are input at the head of tide on a daily basis. Daily loads directly to the tidal system are distributed according to local watershed area. As with runoff, loads from the Susquehanna River provide the major source of nutrients to the main stem bay and these are used to characterize loading during the simulation period. Loads of total nitrogen (TN) and phosphorus mirror the flow pattern (Figure 3). The largest loads during the simulation period occur in the mid-1990s coincident with the largest flows. Due to the dependence of loadings on flow, no long-term trends in loads are apparent. A view of nitrate concentration, the dominant component of nitrogen loads, suggests a dome-shaped trend (Figure 4). Concentrations increase from 1985 to 1990 and remain at the highest levels for that decade. The 2000 decade commences a decreasing trend through the end of the simulation. In an analysis of observed nitrate concentration from 1945 to 2001, Hagy *et al.* (2004) found the peak winter/spring concentration occurred in 1989 and declined thereafter. The WSM results concur with the Hagy *et al.* (2004) timing of peak concentrations, but the WSM decline is delayed relative to the analysis of observations. Phosphate concentration, analogous to nitrate in its availability to phytoplankton, shows a sharp decrease for a decade, from 1993 through 2002, then increases again to the end of the simulation (Figure 4). Winter/spring concentrations at the end of the simulation are similar to the beginning and no trend is apparent.

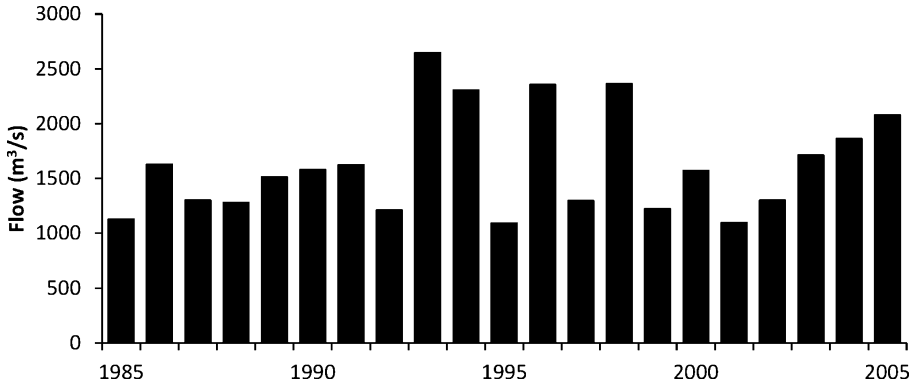

FIGURE 2. Observed Winter-Spring (January-May) Runoff at Conowingo, Situated at the Chesapeake Bay Head of Tide, 1985-2005.

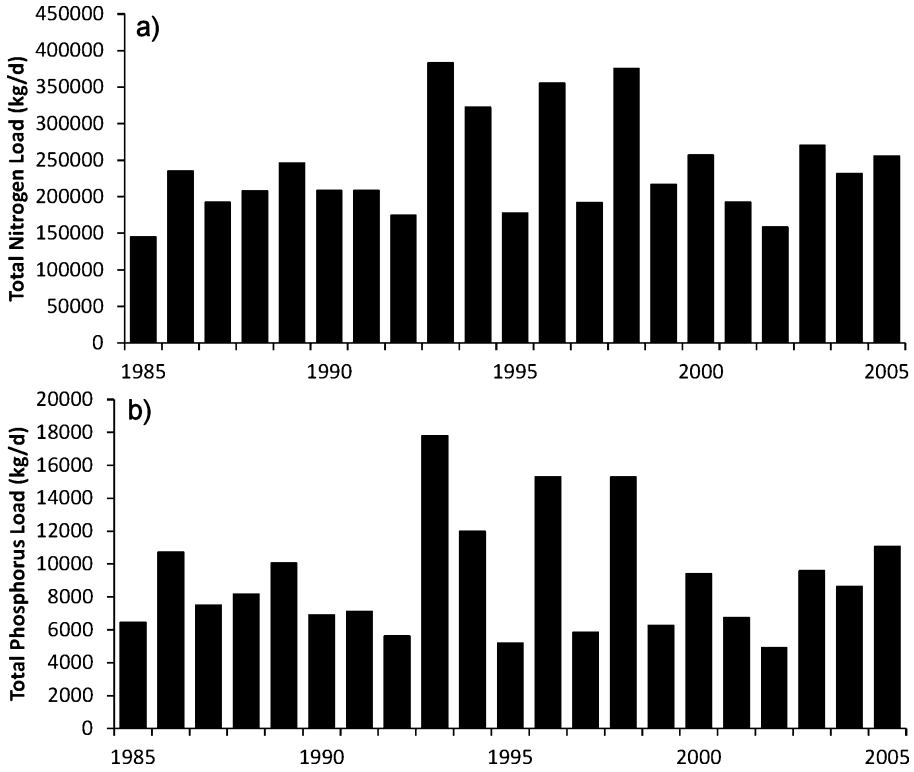

FIGURE 3. Winter-Spring (a) Total Nitrogen and (b) Total Phosphorus Loads at the Chesapeake Bay Head of Tide, as Computed by the Bay Program Watershed Model, 1985-2005.

Stratification

The degree of density stratification in the bay is an important determinant of bottom-water hypoxia. Stratification is characterized here as the surface-to-bottom salinity difference computed at midbay (Station CB5.2, Figure 1) and averaged over the summer months (June-August). Summer stratification (Figure 5) is directly linked to winter/spring runoff; high runoff produces strong stratification ($R^2 = 0.64$) although the relationship is not absolute. Stratification is stronger in 2003 than in 2005 although runoff is greater in 2005. Variations in the relationship of runoff to stratification may originate in the temporal runoff pattern. High flows late in the winter/spring season may produce stronger summer stratification than equivalent flows early in the season. Variations in prevailing winds will also have an effect (Scully, 2010).

Monitoring Program

The CBP operates an extensive monitoring program (CBP Data Hub. Accessed on June 2012. http://www.chesapeakebay.net/dataandtools.aspx) comprising more than 90 stations throughout the system.

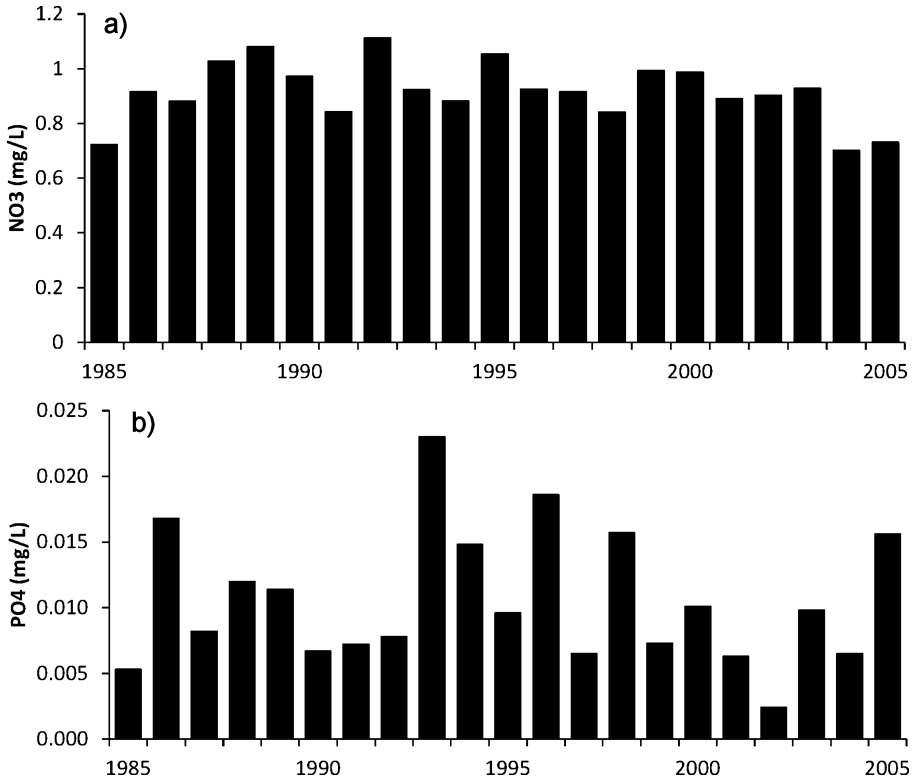

FIGURE 4. Winter-Spring (a) Nitrate and (b) Phosphate Concentration at the Chesapeake Bay Head of Tide, as Computed by the Bay Program Watershed Model, 1985-2005.

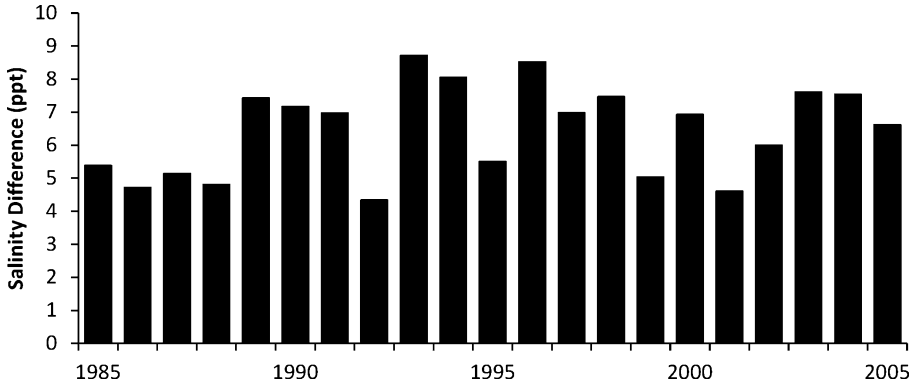

FIGURE 5. Computed Summer-Average Surface-to-Bottom Salinity Difference at Station CB5.2, 1985-2001.

From these, 12 were selected to characterize the main stem bay (Figure 1). These stations are sampled once or twice monthly at various depth intervals. For stratified stations in the main stem, samples for laboratory analysis are collected 1 m below the surface, above the pycnocline, below the pycnocline, and 1 m off the bottom. *In situ* measurements of temperature, salinity, and DO are recorded at 1-m increments. For comparison with the model, laboratory analyses are interpolated at 1-m intervals from surface to bottom and compared with computations in the model surface, mid-depth, and bottom cells. Light attenuation derived from vertical profiles of irradiance is available for different periods depending on station location and monitoring agency. Measures of disk visibility (Secchi depth) have been collected at all stations since commencement of the monitoring program. To form a consistent 21-year record for comparison with the model, light attenuation reported here is derived from the relationship

$$\mathrm{Ke} = 1.4/\mathrm{DV} \tag{1}$$

in which Ke is the diffuse light attenuation (m^{-1}); and DV is the disk visibility (m). This relationship is appropriate for turbid waters (Holmes, 1970) and is

applicable to Chesapeake Bay (Gallegos, 2001) although recent investigations indicate a long-term decline in the product Ke DV (Gallegos *et al.*, 2011).

Comparisons with Observations

The number of measures, analyses, and model variables provides a formidable array of potential comparisons between observations and computations. Comprehensive comparisons in various formats are found in Cerco *et al.* (2010). We focus here on summary graphics and statistics which illustrate overall model performance and then move to long-term trends and behaviors revealed by the model. Emphasis is placed on the variables which relate directly to the water quality impairments (DO, Ke, CHL) and to a limited suite which indicates long-term trends in bay water quality (TN, total phosphorus [TP], total suspended solids [TSS]). Cumulative distribution plots are provided for the 21-year series of observations collected at 12 stations (Figure 1) and multiple depths. Statistical summaries are provided for three statistics over two intervals. The statistics (Cerco and Cole, 1993; Cerco and Noel, 2005) are as follows: mean difference (MD), absolute mean difference (AMD), and relative difference (RD). The first interval, 1985-1986, is utilized to provide statistics for comparison with previous summaries of model performance (Cerco and Noel, 2005). The second interval, 1985-2005, provides a comprehensive summary of present model performance. Time series comparisons of computations and observations are shown for Station CB5.2, situated near the center of the bay (Figure 1).

Spatial and Temporal Aggregation

Detection and illustration of computed trends require aggregation of modeled results in space and time. The main stem of the bay was aggregated into four regions (Figure 1) as well as into one overall result. The regions are aggregations of CBP Segments which are defined based on salinity and physical configuration. The main stem regions were selected to facilitate comparison of model results with a recent analysis of observed trends and behaviors (Williams *et al.*, 2010). CHL, light attenuation (Ke), and TSS, which determine light attenuation were considered in surface cells only. DO, TN, and TP were aggregated into three levels which correspond to the surface mixed layer (Level I, depth < 6.7 m), pycnocline (Level II, 6.7 m < depth < 12.8 m), and mixed bottom waters (Level III, 12.8 m < depth). Daily volumetric averages were determined for each variable over the region and depth interval. Temporal averages were constructed from the daily time series based on periods during which water quality impairments are significant and to facilitate comparisons with published observations. CHL, Ke, TSS, TN, and TP were averaged over the SAV growing season (April-October). DO was averaged over the summer period of bottom-water hypoxia (June-August).

Observed and modeled DO concentrations were summarized to produce a statistic denoted "anoxic volume days" (AVD). The volume of water with observed DO < 1 mg/l was calculated for each sampling cruise (Murphy *et al.*, 2011) using published values of bay bathymetry (Cronin and Pritchard, 1975). For this study, cruise volumes were integrated over time within each modeled year to produce an annual statistic. Similar spatial and temporal summaries were calculated within the model based on cell volumes and concentration calculated at each model time step.

RESULTS

Cumulative Distribution of Observations and Computations

The cumulative distributions of observed and computed CHL are coincident through 90% of the populations (Figure 6a). The 90th percentile of both populations is ≈18 μg/l. The extreme upper end of the observations exceeds 100 μg/l whereas the extreme model values do not exceed 30 μg/l. The distribution of modeled Ke exceeds the observations throughout the range (Figure 6b). At the median, the excess is ≈0.2 m^{-1}. The observed and computed distributions of TSS (Figure 6f) mirror the distributions of Ke and indicate the excess of computed Ke originates with an excess of computed TSS, ≈4 mg/l at the median of modeled and observed distributions. The cumulative distributions of observed and modeled DO (Figure 6c) coincide well through the range from 0 to 16 mg/l. For the most part, the model falls short in TN (Figure 6d); the median of the observations is 0.55 mg/l whereas the median modeled value is 0.45 mg/l. The agreement between observed and modeled distributions of TP is superior to TN (Figure 6e). The distributions are virtually coincident except for a few outlying values (1 or 2% of the populations). The shape of the DO distribution differs from the other substances. Extreme values at the upper end of the DO distribution are absent as the maximum concentration is bounded near the saturation concentration. In contrast, distributions for the other substances, both modeled and observed, exhibit

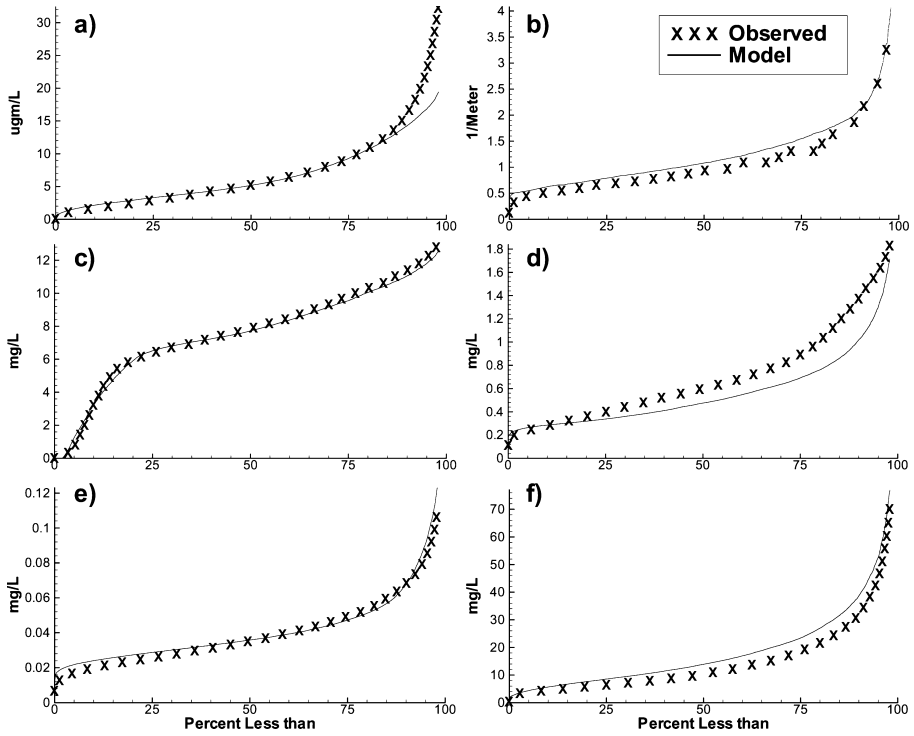

FIGURE 6. Cumulative Distribution Plots of Observed and Computed (a) Chlorophyll, (b) Light Attenuation, (c) Dissolved Oxygen, (d) Total Nitrogen, (e) Total Phosphorus, and (f) Total Suspended Solids. Results are drawn from three depths (except attenuation) at 12 stations sampled monthly over the interval 1985-2005.

sharp upturns to encompass extreme values at the upper end of the distributions. The extreme values in the observations indicate rare occurrences of natural events. The highest modeled values are associated with loading events which are often supplied to the model water column in pulses characterized by extreme concentrations of short duration. In reality, these pulses may be damped by passage of loads through wetlands or vegetation beds at the margins between open water tidal waters and the adjacent land surface.

TABLE 2. Performance Statistics for 21-Year Simulation.

	MD	AMD	RD
Chlorophyll	−0.801	4.09	53.6
Light attenuation	0.233	0.533	47.6
Total nitrogen	−0.124	0.194	27.2
Total phosphorus	0.002	0.017	40.9
Dissolved oxygen	−0.081	1.04	13.5
Total suspended solids	3.95	12.2	76.7

Notes: MD, mean difference; AMD, absolute mean difference; RD, relative difference. Chlorophyll MD and AMD in μg/l. Light attenuation MD and AMD in 1/m. All others in mg/l. RD in percent for all substances.
MD > 0 indicates model computation exceeds observations on average.

Statistical Summary

A wide range of model performance statistics can be employed. The statistics employed here (MD, AMD, RD) are selected to provide a consistent series dating back to the original Chesapeake Bay application of this model (Cerco and Cole, 1993). The statistics for the 21-year simulation (Table 2) reflect the graphical summaries and previous experience. Computed TSS and Ke exceed observations, on average, whereas observed TN exceeds modeled values. The MD statistic also reveals differences in average CHL, TP, and DO that are not apparent in the distribution plots. The RD statistic indicates DO computations are overall the most accurate. We attribute the relative accuracy to the physical processes which limit and partially determine the concentration. The least accurate computations are CHL and TSS. CHL is a biotic component with no upper boundary on concentration. The majority of TSS is inert, but accurate computation requires simultaneous accurate calculations of loading, physical processes, and biological production of the organic solids fraction. The remaining substances (Ke, TN, TP) occupy a mid-range of relative accuracy.

Statistical summaries were repeated (Table 3) using only observations from the years 1985-1986 to provide consistency with previous summaries (Cerco and Noel, 2005). To provide consistency with previous

TABLE 3. Performance Statistics for Four Model Phases: (1) the Original Version Created for the Reevaluation of the 1987 Nutrient Reduction Goals; (2) the Version with Improved Resolution and Living Resources Employed for Virginia Tributary Refinements; (3) the 2003 Version with Further Improved Resolution; and (4) the Present Version. Comparisons are restricted to model years 1985-1986 to provide consistency among versions and with previously published statistics. See text for details.

	Phase 1	Phase 2	Phase 3	Phase 4
Chlorophyll				
MD	1.55	1.52	0.32	1.35
AMD	4.97	4.9	5.01	4.53
RD	61.6	57.6	59.2	66
Light attenuation				
MD	0.085	0.147	−0.065	0.07
AMD	0.367	0.469	0.36	0.461
RD	36.5	45.2	38.5	44.5
Total nitrogen				
MD	−0.002	−0.023	−0.025	−0.15
AMD	0.149	0.143	0.17	0.192
RD	22.1	21.3	21.9	27.1
Total phosphorus				
MD	−0.014	−0.011	−0.012	−0.008
AMD	0.018	0.017	0.014	0.022
RD	42.5	38.5	41.5	44.3
Dissolved oxygen				
MD	0.775	−0.522	0.03	0.221
AMD	1.94	1.362	1.47	1.24
RD	44.9	31.6	27.9	27.7

Notes: MD, mean difference; AMD, absolute mean difference; RD, relative difference. Chlorophyll MD and AMD in μg/l. Light attenuation MD and AMD in 1/m. All others in mg/l. RD in percent for all substances.
MD > 0 indicates model computation exceeds observations on average.

DO statistics, comparisons were limited to observations collected during summer at the bottom of the water column. This restriction coincides with the period of hypoxia and emphasizes computations that depend on processes including respiration and stratification. Saturated surface concentrations which rely largely on the computation of temperature are not considered. Under this limitation, AMD is nearly 25% higher and RD is double the value obtained when the population of DO observations is considered.

DO is perhaps the only substance which shows a consistent improvement due to grid refinements and model developments. On average, computed TN and TP concentrations have been low since the inception of the modeling effort while computed CHL has been high. Cerco and Cole (1993) suggested that the MD statistic for phosphorus indicates a missing source, likely particle-bound phosphorus associated with bank erosion. No explicit reason can be offered for the consistent average differences in CHL and TN. We note, however, that the model is calibrated based on visual inspection of model results. A calibration aimed at optimizing performance statistics might improve on the results shown. Absence of consistent improvement in computations of multiple substances has been noted previously (Cerco and Noel, 2005). Model improvements have added capability rather than accuracy. Grid refinements have pushed the model into regions of smaller and smaller extent. Refinements to the algorithms for light attenuation and TSS (Cerco *et al.*, 2010) have improved realism and reduced the amount of human judgment involved in computing these constituents. To an extent, removal of judgment and freedom to arbitrarily adjust parameters adversely affects model performance. Maintaining performance statistics while increasing model rigor is, in fact, an overall improvement in the model.

Time Series

Selected time series comparisons of computed and observed properties (Figure 7) are presented at station CB5.2 (Figure 1). The station is situated in open water near the center of the bay and demonstrates typical behavior including bottom-water hypoxia. More extensive comparisons may be found in Cerco *et al.* (2010). Careful inspection of the modeled surface CHL concentration (Figure 7a) indicates two peaks each year. The first, higher peak is the spring diatom bloom and the second, lower peak corresponds to the summer period of maximum productivity (Malone *et al.*, 1988; Miller and Harding, 2007). These annual occurrences are difficult to discern in the observations. The model encompasses the majority of the CHL observations although extreme outliers occur that are not captured. The model is highly accurate in reproducing the recurring annual summer anoxia as well as the saturated concentrations which occur during the cooler, well-mixed periods (Figure 7c). Light attenuation (Figure 7b) is perhaps the only measure considered here which shows a clear trend. Observations increase over the simulation period due to a trend of decreasing disk visibility (Williams *et al.*, 2010). Whether the decreasing disk visibility truly indicates increasing attenuation has recently been called into question (Gallegos *et al.*, 2011). Our model is not capable of addressing this issue. However, the model clearly shows higher variability and the highest computed values of attenuation in the latter half of the record. Observed TN concentrations (Figure 7d) fluctuate widely, due to runoff events. The highest observations occur in the mid-1990s and in the last three years of the record, reflecting high runoff in those same years (Figure 2). Although the model reflects the flow events as well, the magnitude of the observed peaks is not reproduced, perhaps indicating that modeled losses of TN

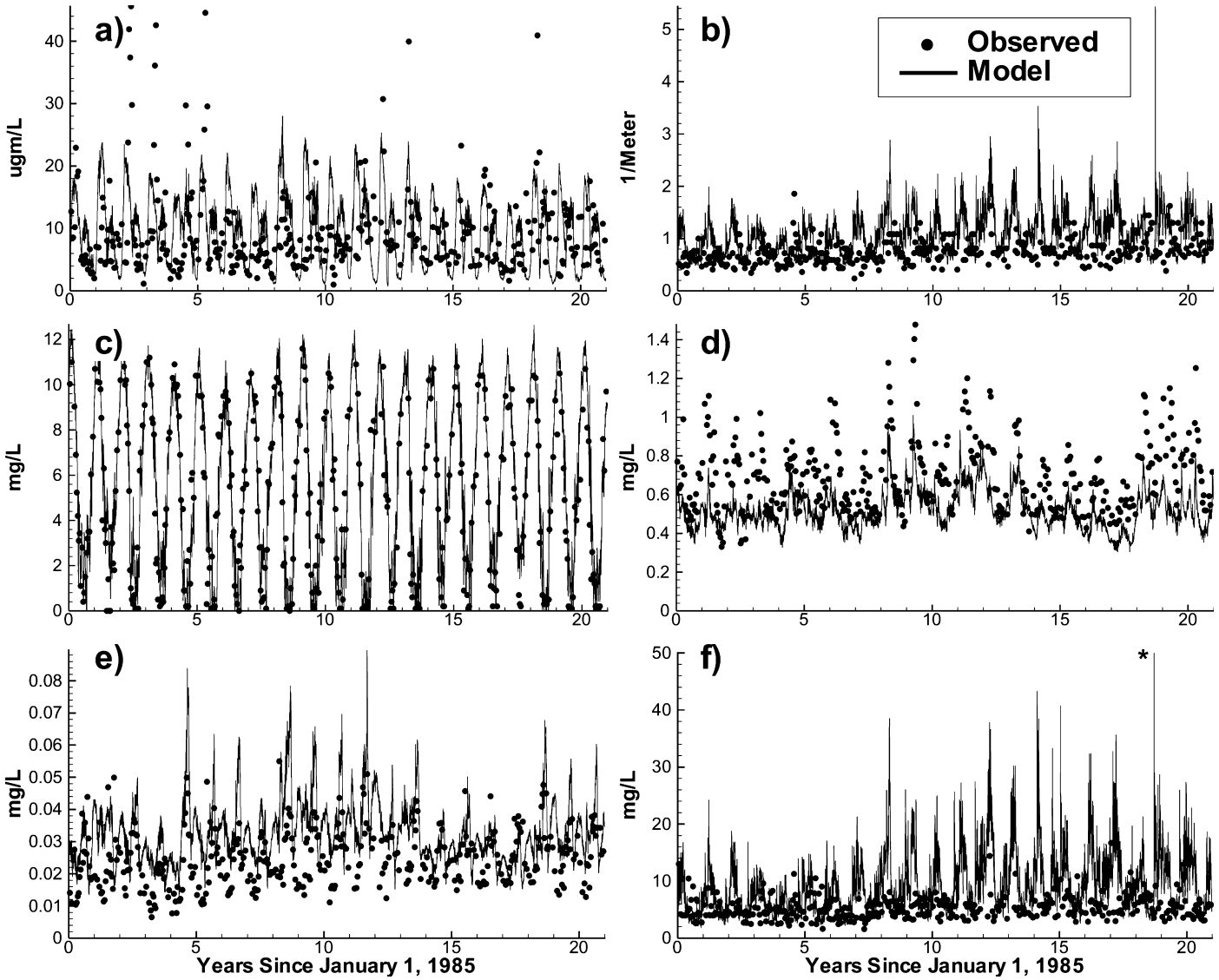

FIGURE 7. Time Series Comparisons of Observed and Computed (a) Surface Chlorophyll, (b) Light Attenuation, (c) Bottom Dissolved Oxygen, (d) Surface Total Nitrogen, (e) Surface Total Phosphorus, and (f) Surface Total Suspended Solids (TSS) at Station CB5.2, Located Near the Center of Chesapeake Bay. (*) Indicates TSS concentration of 90 mg/l.

from the water column are exaggerated. A shortfall in loading is also possible. Variability in the observed TP confounds interpretation of trends and events, although there is some evidence of the mid-1990s and 2003-2005 runoff events (Figure 7e). Variability in modeled TP is produced by two phenomena: runoff events and sediment phosphorus release during periods of bottom-water anoxia (Boynton and Kemp, 1985; DiToro, 2001). Higher concentrations during the mid-1990s and 2003-2005 runoff events are obvious. Inspection of phosphorus peaks, however, indicates that they occur in late summer and indicate diffusion of phosphorus from deep, anoxic water rather than loads from upstream. The years with the highest computed TP, 1989 and 1996, are the years with the greatest computed anoxic volume. Additional discussion of this connection follows in a subsequent section. Observed TSS are limited to a range of $\approx$10 mg/l and show little connection to runoff events (Figure 7f). The model, in contrast, shows high variability and excess concentrations, especially during the second half of the record. Modeled TSS at this location is influenced by multiple factors including loading, circulation, deposition, and resuspension. The factor (or combination of factors) that causes the excess in computed TSS is not obvious.

Modeled Trends

Intermittent surveys of Chesapeake Bay extend back into the 1930s (CBI Water Quality Database

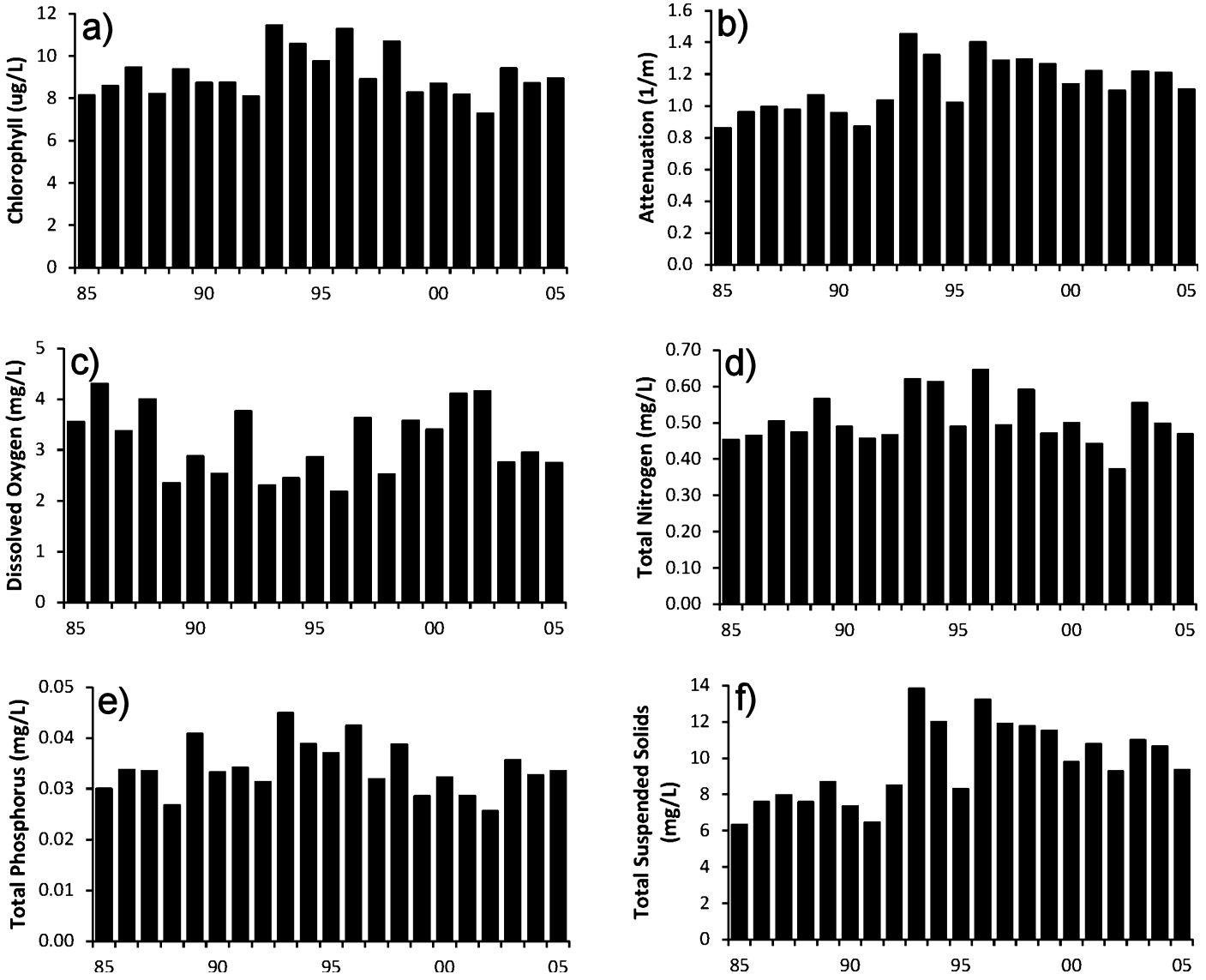

FIGURE 8. Bay-Wide Trends in Computed (a) Surface Chlorophyll, (b) Light Attenuation, (c) Level III Dissolved Oxygen (DO), (d) Level I Total Nitrogen, (e) Level I Total Phosphorus, and (f) Surface Total Suspended Solids. Surface results are from depths <2 m. Level I results represent the surface mixed layer, up to 6.7 m deep. Level III results are from bottom water, depth >12.8 m. DO is from the period of summer bottom-water hypoxia (June-August). All others from the submerged aquatic vegetation growing season (April-October).

(1949-1982). Accessed on June 2012. http://www.chesapeakebay.net/data/downloads/cbi_water_quality_database_1949_1982). Intensive, regular monitoring commenced in late 1984 with the inception of the U.S. Environmental Protection Agency CBP. Multiple publications in recent years (Hagy *et al.*, 2004; Prasad *et al.*, 2010; Williams *et al.*, 2010; Murphy *et al.*, 2011) have examined the data record, identified trends, and ascribed causes to the trends. Detection of trends in observed time series is difficult and subject to interpretation due to data gaps, inherent variability, superposition of multiple forcing functions, and the potential influence of unknown factors. Trend detection in the model is easier as the model record is complete. Computed concentrations are known throughout the system at all times. The forcing functions are known exactly although the interpretation of multiple forcings with different recurrences can still be daunting. In view of the recent examinations and interpretations of the observed record, we concentrate here on interpretation of the modeled trends and comparison with recent reports.

Computed surface CHL (Figure 8a) shows the highest values in the mid-1990s, corresponding closely to the years with the highest TN concentration and the greatest winter-spring TN loading (Figure 3). Concentrations prior to the high-loading years (1993-1998) and after are roughly equivalent and show no trend. Computed Ke (Figure 8b) increases sharply in 1993 relative to the preceding years. Although flows

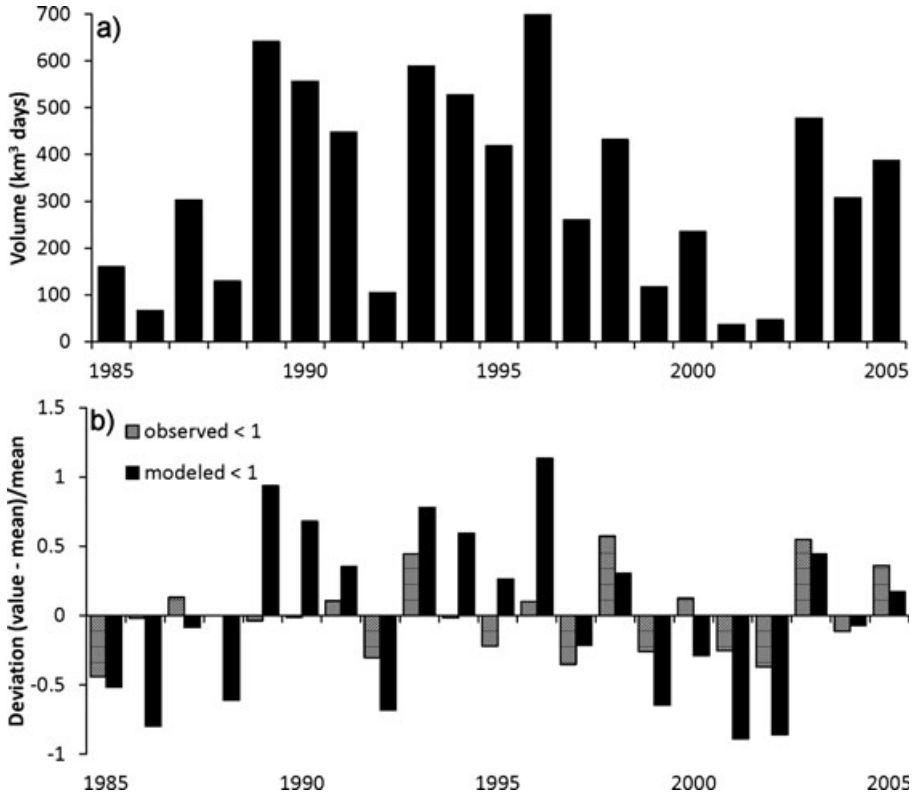

FIGURE 9. (a) Computed Annual Anoxic Volume Days (AVD) in the Chesapeake Bay Main Stem, 1985-2005. AVD are a spatial and temporal integral of the volume of water with dissolved oxygen less than 1 mg/l. (b) Observed and computed annual deviation from mean AVD.

decline to some of the lowest values in the sequence, in 1999 and 2001, Ke never recovers its pre-1993 values. This pattern in Ke is linked to a similar pattern in surface TSS. The high-flow years (Figure 2) influence the TN and TP concentrations; the highest concentrations predominantly occur during the years with the highest flows.

No temporal trends are apparent in computed bottom-water DO (Figure 8c) or AVD (Figure 9a) although a relationship between runoff and AVD is apparent. Large volumes are computed in 1993 and 1996, years of high runoff. Small volumes computed in 1982 and 2001 correspond to low runoff. The apparent correlations are not universal, however. Anomalously large and small volumes are computed in 1986 and 1989, years of comparable, moderate runoff. Computed annual AVD is correlated with observed ($R^2 = 0.31$, $p = 0.01$). One-to-one comparisons with observed AVD are confounded, however, by the interpolations and extrapolations necessary to integrate the observations over the bay volume and by differences in bay volume determined by bathymetry and by model grid. The influence of different bay volumes was eliminated by normalizing the observed and modeled AVD by the mean values and examining the excursion from long-term mean value in each model year (Figure 9b). The result demonstrates consistency between the observed deviations from mean and modeled deviations. Observed excursions above or below mean tend to be matched by modeled deviations. The model demonstrates much greater variability about the mean than the observations, however.

Examination of model results reveals few monotonic trends, but numerous patterns and associations. The significance of patterns and potential cause-and-effect relationships were examined via linear regression. Model results (surface CHL, Ke, surface TSS, Level III DO, Level I and III TN, Level I and III TP) were regressed against causative factors (TN load, NO_3 load, TP load, PO_4 load, annual AVD, midbay stratification) using stepwise regression (SAS 9.3, http://www.sas.com/software/sas9/) with variables entered in order of significance ($p < 0.15$). Loads were considered at the Susquehanna fall line (Figure 1). Regressions were performed for individual segments (Figure 1) and overall.

In most cases, results from individual segments reflected overall results although significant regional differences were noted for surface CHL. The best predictor of bay-wide surface CHL is TN load ($R^2 = 0.74$, Table 4). In the upper bay (segments CB1-3), however, the best predictors of surface CHL are AVD

TABLE 4. Results of Linear Regression to Examine Cause-and-Effect Relationships in Model Behavior. Variables entered in stepwise regression ($p < 0.15$). Independent variables are listed in the top row and dependent variables are listed in the first column. Delta S is the bottom-surface salinity. Delta Snorm is Delta S divided by the mean salinity.

			Q (m^3/s)	**TN load (kg/d)**	**NO_3 load (kg/d)**	**TP load (kg/d)**	**PO_4 load (kg/d)**	**AVD (km^3 d)**	**Delta S (ppt)**	**Delta Snorm**
Bay-wide surface CHL (μg/l)	Intercept	7.14								
	Coefficient			2.21×10^{-6}			4.3×10^{-4}	2.27×10^{-3}		
	Partial R^2			0.74			0.0265	0.0993		
Bay-wide Ke (1/m)	Intercept	0.436								
	Coefficient		-1.99×10^{-4}		5.7×10^{-6}			-4.89×10^{-4}		1.27
	Partial R^2		0.054		0.617			0.055		0.071
Bay-wide surface TSS (mg/l)	Intercept	0.758								
	Coefficient		-2.57×10^{-3}		7.38×10^{-5}			-6.36×10^{-3}		16.33
	Partial R^2		0.054		0.613			0.057		0.0704
DO (mg/l), depth >12.8 m	Intercept	5.81								
	Coefficient								−0.411	
	Partial R^2								0.688	
Bay-wide TN (mg/l), surface mixed layer	Intercept	0.329								
	Coefficient		-7.89×10^{-5}	1.07×10^{-6}				1.49×10^{-4}		
	Partial R^2		0.038	0.762				0.094		
Bay-wide TN (mg/l), depth >12.8 m	Intercept	0.308								
	Coefficient			5.98×10^{-7}				1.48×10^{-4}		
	Partial R^2			0.73				0.109		
Bay-wide TP (mg/l), surface mixed layer	Intercept	0.0264								
	Coefficient					1.83×10^{-6}		1.43×10^{-5}		
	Partial R^2					0.129		0.739		
Bay-wide TP (mg/l), depth >12.8 m	Intercept	0.0332								
	Coefficient					2.56×10^{-6}		3.36×10^{-5}		
	Partial R^2					0.066		0.816		
Surface CHL (μg/l) CBP segments 1-3	Intercept	11.1								
	Coefficient							4.08×10^{-3}		−11.34
	Partial R^2							0.287		0.197
Surface CHL (μg/l), CBP segments 4-5	Intercept	10.4								
	Coefficient		-1.45×10^{-3}				1.07×10^{-3}	3.54×10^{-3}		
	Partial R^2		0.036				0.698	0.14		
Surface CHL (μg/l), CBP segments 6-8	Intercept	3.62								
	Coefficient				2.97×10^{-5}			1.55×10^{-3}		
	Partial R^2				0.788			0.034		
Surface CHL (μg/l), CBP segment TANMH	Intercept	5.49								
	Coefficient			1.06×10^{-5}				2.39×10^{-3}		
	Partial R^2			0.684				0.09		

Notes: Q, Flow; TN, Total Nitrogen; TP, Total Phosphorus; AVD, Anoxic Volume Days; DO, Dissolved Oxygen; CHL, Chlorophyll. See Figure 1 for locations of CBP and TANMH.

(R^2 = 0.287, Table 4) and Delta Snorm, a normalized measure of stratification (R^2 = 0.197, Table 4). The regression results indicate associations but not necessarily cause-and-effect relationships. We interpret these results as follows. The positive relationship with AVD is indicative of anoxia-induced nutrient releases (Boynton and Kemp, 1985; DiToro, 2001) which support CHL production in the upper bay. The stratification measure reflects flow; high runoff induces high stratification while low runoff minimizes stratification. The negative relationship with stratification reflects a negative relationship with flow. CHL is higher during low-flow periods. Flow itself does not figure in the regressions, perhaps because the relationship between upper bay CHL and flow is nonlinear. Moving down the bay, surface CHL in segments CB4-5 is best predicted by PO_4 load (R^2 = 0.698, Table 4) whereas surface CHL in the lower bay, segments CB6-8 and TANMH, is best predicted by NO_3 or TN load (R^2 = 0.788 and 0.684, respectively, Table 4). The results from individual segments indicate a model progression in influences on CHL, from physical factors in the upper bay to phosphorus loads in midbay, to nitrogen loads in the lower bay.

Baywide KE and TSS are best predicted as functions of NO_3 load (R^2 = 0.617 and 0.613, respectively, Table 4). The relationship reflects the origin of suspended particulate matter in primary production of particles which is stimulated by nitrogen loading. TN concentration is, of course, related to TN loading (R^2 = 0.73 to 0.76, Table 4) although a secondary relationship with AVD exists (R^2 = 0.094 to 0.109, Table 4), indicating the role of sediment nitrogen release during anoxic intervals. Sediment nutrient release is a prominent influence on TP concentration in both surface and bottom waters as indicated by the predictive relationship between AVD and TP (R^2 = 0.739 to 0.816, Table 4). TP load provides supplementary predictive capability to AVD (R^2 = 0.066 to 0.129, Table 4). The relative importance of loading *vs*. sediment nutrient release is reversed when examining TN and TP. The primary predictor of Level III DO is stratification, expressed as surface-to-bottom salinity difference. The relationship is strong (R^2 = 0.688) and negative. High stratification induces low bottom-water DO whereas low stratification permits high bottom-water DO concentrations.

DISCUSSION

Our 21-year simulation shows few monotonic trends. The modeled bay is neither improving nor deteriorating, with one exception. Light attenuation post-1993 is greater than the earlier period. The pattern in computed light attenuation is the same as surface TSS, which are a major component in attenuation. Regression analysis indicates that model TSS are related to NO_3 loading. Nitrogen loads stimulate phytoplankton production and the production of particulate organic matter which comprises a significant fraction of TSS (Cerco *et al.*, 2012). Williams *et al.* (2010) found that disk visibility was deteriorating in multiple regions of the bay, reflecting our model results. They attributed the deterioration to increased annual flow post-1992 and development in the coastal plain watershed. Our model reflects increased flows as increased loads (Figures 2 and 3) although we indicated NO_3 concentration is lately declining. The decline in concentration is overwhelmed by the flow effect, however.

Analysis of model relationships indicates a progression of dominant influences on surface CHL. In the upper bay, physical factors are most important. Low runoff from the watershed promotes surface CHL by increasing residence time whereas higher runoff dilutes surface CHL concentration and decreases residence time. However, influences from runoff are confounding. Higher runoff induces stratification which promotes bottom-water anoxia and sediment nutrient releases which stimulate algal production. Further down the bay, influences on surface CHL transition from P loads to N loads. Overall, N loads are most influential on CHL. The relative importance of P *vs*. N loads agrees with research and paradigms regarding the roles of nutrients in Chesapeake Bay phytoplankton production (Fisher *et al.*, 1992; Malone *et al.*, 1996).

The strongest predictor of model bottom-water DO concentration is stratification. This result is analogous to Hagy *et al.* (2004) who found that the only predictor of hypoxic volume in the years 1985-2001 was winter-spring river flow. Hagy *et al.* also noted the presence of inherent and unexplained variability in the record of hypoxic volume. The year with the greatest nutrient loads in their examined sequence (1996) had less hypoxic volume than the preceding low-flow year. The modeled record indicates a relationship between hypoxic volume and flow, but contains anomalies as well.

We do not claim that nutrient loads from the watershed are unimportant in determining hypoxia. Rather, we find that the variation in loads over the model application period is small relative to the changes required to induce major improvements in water quality. Our findings are consistent with Hagy *et al.* (2004) who related changes in hypoxia over 50 years to changes in loads, but were unable to detect the influence of loads in the interval 1985-2001. We also note that recent work (Murphy *et al.*, 2011) indicates that early-summer hypoxia is related to

stratification whereas late-summer hypoxia is related to loads. Our analysis of annual AVD does not parse out these potential relationships in the model.

The model indicates that the TN concentration in the bay is largely influenced by loads with a secondary influence of anoxic volume which induces sediment nutrient releases. The roles of loads *vs*. hypoxia are reversed for TP concentration. Our results are similar to Prasad *et al.* (2010) who found that a significant fraction of variation in bay dissolved inorganic nitrogen was related to river loads whereas only 5% of the variation in bay PO_4 could be related to loads. They attributed the weak connection between PO_4 concentration and PO_4 loads to release from sediments.

Our methodology must be considered when interpreting our results. We used linear regression, with variables entered stepwise, to relate forcing factors (e.g., loading) to effects (e.g., CHL concentration). In the analysis of bottom-water DO concentration, the strongest linear predictor of DO is stratification ($R^2 = 0.688$). Our results do not imply that bottom-water DO is unrelated to TN load or, potentially, other factors. The correlation between bottom-water DO and TN loading, $R^2 = 0.46$ is strong. Once stratification is incorporated in the regression, however, the additional predictive power added by TN load is insignificant. Although we distinguish causative factors and results, these cannot always be separated. Hypoxia induces sediment nutrient releases which stimulate algal production. Deposition of algal organic matter enhances hypoxia and further stimulates nutrient releases. Finally, nonlinear predictive relationships may exist and escape notice in linear regression.

Results of our model examination emphasize the influence of physical factors (runoff, stratification) on water quality. Stratification is the most significant influence on bottom-water DO. Hypoxia, induced by stratification, has the strongest correlation with modeled TP concentration. AVD and stratification (a surrogate for runoff) are the primary determinants of upper bay CHL. Our emphasis on physics parallels recent work (Scully, 2010), which emphasizes the role of climate patterns and wind direction on hypoxia. Although our work does not specifically examine climatic influences on hypoxia, both works stress the role of physics in bay water quality.

SUMMARY AND CONCLUSIONS

We have created a 21-year simulation of eutrophication processes in Chesapeake Bay and tributaries. Modeled eutrophication processes are determined by internal transformations of modeled substances and by external forcing factors. One forcing factor is the CBP WSM (Shenk and Linker, this issue) which provides nutrient and solids loads. Computed trends (or lack of trends) in the eutrophication model reflect loading trends in the WSM. Hydrodynamics from the CH3D hydrodynamic model (Kim, this issue) provide a second set of external forces. Hydrodynamics are, in turn, determined by runoff from the watershed and climatic factors including wind. We introduced several new features to the eutrophication model, notably a rigorous optical model and resuspension of suspended solids. Model accuracy is comparable with previous applications with improvements noted in terms of model capacity and management utility. Our model displays few long-term trends in water quality although multiple patterns and relationships are revealed. The most significant result is the influence of physical processes, notable stratification, and associated effects (e.g., anoxic volume) on water quality. Within the application period, physical effects are more important determinants of year-to-year variability in water quality than external loads.

ACKNOWLEDGMENTS

This study was funded by the US Army Engineer District, Baltimore, and by the US Environmental Protection Agency Chesapeake Bay Program Office. Rebecca Murphy provided the anoxic volumes for individual sampling cruises. US Environmental Protection Agency publication EPA-903-R-13-011, Chesapeake Bay program publication CBP/TRS-317-13-10.

LITERATURE CITED

Boynton, W. and W. Kemp, 1985. Nutrient Regeneration and Oxygen Consumption Along an Estuarine Salinity Gradient. Marine Ecology Progress Series 23:45-55.

Butt, A.J., L.C. Linker, J.S. Sweeney, G.W. Shenk, R.A. Batiuk, and C.F. Cerco, 2000. Technical Tools Used in the Development of Virginia's Tributary Strategies: A Synthesis of Airshed, Watershed, and Estuary Model Results. A Technical Summary Report. September, 2000. Department of Environmental Quality, Richmond Virginia. http://www.chesapeakebay.net/publications/title/technical_tools_used_in_the_development_of_virginias_tributary_strategies_a, *accessed* July 2013.

CBP (Chesapeake Bay Program), 1987. The 1987 Chesapeake Bay Agreement. http://www.chesapeakebay.net/publications/title/chesapeake_bay_agreement_-_1987, *accessed* July 2013.

Cerco, C. and T. Cole, 1993. Three-Dimensional Eutrophication Model of Chesapeake Bay. Journal of Environmental Engineering 119(6):1006-1025.

Cerco, C., S.-C. Kim, and M. Noel, 2010. The 2010 Chesapeake Bay Eutrophication Model. A Report to the US Environmental Protection Agency Chesapeake Bay Program and to the US Army Engineer Baltimore District. http://www.chesapeakebay.net/publications/title/the_2010_chesapeake_bay_eutrophication_model1, *accessed* July 2013.

Cerco, C., S.-C. Kim, and M. Noel, 2012. Management Modeling of Suspended Solids in the Chesapeake Bay, USA. Estuarine, Coastal and Shelf Science 116:87-98.

Cerco, C., L. Linker, J. Sweeney, G. Shenk, and A. Butt, 2002. Nutrient and Solids Controls in Virginia's Chesapeake Bay Tributaries. Journal of Water Resources Planning and Management 128(3):179-189.

Cerco, C. and M. Meyers, 2000. Tributary Refinements to the Chesapeake Bay Model. Journal of Environmental Engineering 126(2):164-174.

Cerco, C. and K. Moore, 2001. System-Wide Submerged Aquatic Vegetation Model for Chesapeake Bay. Estuaries 24(4):522-534.

Cerco, C. and M. Noel, 2004. The 2002 Chesapeake Bay Eutrophication Model. US Environmental Protection Agency Chesapeake Bay Program Office, Annapolis, Maryland. EPA 903-R-04-004. http://www.chesapeakebay.net/publications/title/the_2002_chesapeake_bay_eutrophication_model, *accessed* July 2013.

Cerco, C. and M. Noel, 2005. Incremental Improvements in Chesapeake Bay Environmental Model Package. Journal of Environmental Engineering 131(5):745-754.

Cerco, C., M. Noel, and L. Linker, 2004. Managing for Water Clarity in Chesapeake Bay. Journal of Environmental Engineering 130(6):631-642.

Cronin, W. and D. Pritchard, 1975. Additional Statistics of Chesapeake Bay and Its Tributaries: Cross-Section Widths and Segment Volumes per Meter Depth. Reference 75-3. Special Report 42. Chesapeake Bay Institute, The Johns Hopkins University, Baltimore, Maryland.

Dennis, R.L., R. Mathur, J. Pleim, and J. Walker, 2010. Fate of Ammonia Emissions at the Local to Regional Scale as Simulated by the Community Multiscale Air Quality Model. Atmospheric Pollution Research 1(4): 207-214, doi: 10.5094/APR.2010.027.

DiToro, D., 2001. Sediment Flux Modeling. John Wiley and Sons, New York City, New York, ISBN 0-471-13535-6.

Fisher, T., E. Peele, J. Ammerman, and L. Harding, 1992. Nutrient Limitation of Phytoplankton in Chesapeake Bay. Marine Ecology Progress Series 82:51-63.

Gallegos, C., 2001. Calculating Optical Water Quality Targets to Restore and Protect Submerged Aquatic Vegetation: Overcoming Problems in Partitioning the Diffuse Attenuation Coefficient for Photosynthetically Active Radiation. Estuaries 24(3):381-397.

Gallegos, C.L., P.J. Werdell, and C.R. McClain, 2011. Long-Term Changes in Light Scattering in Chesapeake Bay Inferred from Secchi Depth, Light Attenuation, and Remote Sensing Measurements. Journal of Geophysical Research 117:1-19, doi: 10.1029/JC2011007160.

Grimm, J. and J. Lynch, 2004. Enhanced Wet Deposition Estimates Using Modeled Precipitation Inputs. Environmental Monitoring and Assessment 90:243-268.

Hagy, J., W. Boynton, C. Keefe, and K. Wood, 2004. Hypoxia in Chesapeake Bay, 1950–2001: Long-Term Change in Relation to Nutrient Loading and River Flow. Estuaries 27(4):634-658.

Holmes, R., 1970. The Secchi Disk in Turbid Coastal Water. Limnology and Oceanography 15:688-694.

HydroQual Inc., 1987. A Steady-State Coupled Hydrodynamic/Water Quality Model of the Eutrophication and Anoxia Process in Chesapeake Bay. Work Assignment No. 40, EPA Contract No. 68-03-3319. Prepared by HydroQual Inc. under contract to Battelle Ocean Sciences for the US Environmetnal Protection Agency Chesapeake Bay Program, Annapolis, Maryland.

Kim, S.-C., this issue. Evaluation of a Three-Dimensional Hydrodynamic Model Applied to Chesapeake Bay Through Long-Term Simulation of Transport Processes. Journal of the American Water Resources Association, doi: 10.1111/jawr.12113. EPA-903-R-13-006. CBP/TRS-312-13-5.

Malone, T.C., D.J. Conley, T.R. Fisher, P.M. Glibert, and L.W. Harding, Jr., 1996. Scales of Nutrient Limited Phytoplankton Productivity in Chesapeake Bay. Estuaries 19:371-385.

Malone, T.C., L.H. Crocker, S.E. Pike, and B.W. Wendler, 1988. Influences of River Flow on the Dynamics of Phytoplankton Production in a Partially Stratified Estuary. Marine Ecology Progress Series 48:235-249.

Miller, W.D. and L. Harding, Jr., 2007. Climate Forcing of the Spring Bloom in Chesapeake Bay. Marine Ecology Progress Series 331: 11-22.

Murphy, R., W. Kemp, and W. Ball, 2011. Long-Term Trends in Chesapeake Bay Seasonal Hypoxia, Stratification, and Nutrient Loading. Estuaries and Coasts 34:1293-1309, doi: 10.1007/s12237-011-9413-7.

Prasad, M., M. Sapiano, C. Anderson, W. Long, and R. Murtugudde, 2010. Long-Term Variability of Nutrients and Chlorophyll in the Chesapeake Bay: A Retrospective Analysis, 1985-2008. Estuaries and Coasts 33:1128-1143, doi: 10.1007/s12237-010-9325-y.

Scully, M., 2010. The Importance of Climate Variability to Wind-Driven Modulation of Hypoxia in Chesapeake Bay. Journal of Physical Oceanography 40:1435-1440, doi: 10.1175/2010JPO4321.1.

Shenk, G.W. and L.C. Linker, this issue. Development and Application of the 2010 Chesapeake Bay Watershed Total Maximum Daily Load Model. Journal of the American Water Resources Association, doi: 10.1111/jawr.12109. EPA-903-R-13-004. CBP/TRS-310-13-3.

USEPA (U.S. Environmental Protection Agency), 2003. Ambient Water Quality Criteria for Dissolved Oxygen, Water Clarity and Chlorophyll a for the Chesapeake Bay and Its Tidal Tributaries. EPA 903-R-03-002. U.S. Environmental Protection Agency, Region 3, Chesapeake Bay Program Office, Annapolis, Maryland.

USEPA (U.S. Environmental Protection Agency), 2010. Chesapeake Bay Total Maximum Daily Load for Nitrogen, Phosphorus, and Sediment. U.S. Environmental Protection Agency, Region 3, Philadelphia, Pennsylvania.

Williams, M., S. Filoso, B. Longstaff, and W. Dennison, 2010. Long-Term Trends of Water Quality and Biotic Metrics in Chesapeake Bay: 1986 to 2008. Estuaries and Coasts 33:1279-1299, doi: 10.1007/s12237-010-9333-y.